

## Research Article

# Antiviral Effect of Hyunggaeyungyo-Tang on A549 Cells Infected with Human Coronavirus

Seo-Young Won <sup>1,2</sup>, In-Chan Seol <sup>1,3</sup>, Ho-Ryong Yoo <sup>1,3</sup> and Yoon-Sik Kim <sup>1,2</sup>

<sup>1</sup>Department of Korean Internal Medicine, College of Korean Medicine Daejeon University, Daejeon KS015, Republic of Korea

<sup>2</sup>Department of Korean Internal Medicine, Cheonan Korean Medicine Hospital of Daejeon University, Cheonan-Si KS002, Republic of Korea

<sup>3</sup>Department of Korean Internal Medicine, Daejeon Korean Medicine Hospital of Daejeon University, Daejeon KS015, Republic of Korea

Correspondence should be addressed to Yoon-Sik Kim; [yoonsik@dju.kr](mailto:yoonsik@dju.kr)

Received 17 May 2021; Revised 8 July 2021; Accepted 30 August 2021; Published 6 October 2021

Academic Editor: Yu Hsiang Kuan

Copyright © 2021 Seo-Young Won et al. This is an open access article distributed under the Creative Commons Attribution License, which permits unrestricted use, distribution, and reproduction in any medium, provided the original work is properly cited.

**Background.** Herbal medicine is widely recommended to treat viral infectious diseases. Over 123,000,000 individuals have been infected with the coronavirus since a worldwide pandemic was declared in March 2020. We conducted this research to confirm the potential of herbal medicine as a treatment for coronavirus. **Methods.** We infected the A549 cell line with betacoronavirus OC43 and then treated it with 100 µg/mL Hyunggaeyungyo-tang (HGYGT) or distilled water with a control of HGYGT. We measured the mRNA expression levels of proinflammatory cytokines and interferon stimulated genes (ISGs) to confirm the effectiveness of HGYGT upon coronavirus infection. **Results.** We found that the effects of HGYGT decrease the expression level of pPKR, peIF2α, IFI6, IFI44, IFI44L, IFI27, IRF7, OASL, and ISG15 when administered to cells with coronavirus infection. The expressions of IL-1, TNF-α, COX-2, NF-κB, iNOS, and IKK mRNA were also significantly decreased in the HGYGT group than in the control group. **Conclusion.** Through the reduction of the amount of coronavirus RNA, our research indicates that HGYGT has antiviral effects. The reduction of IKK and iNOS mRNA levels indicate that HGYGT reduces coronavirus RNA expression and may inhibit the replication of coronavirus by acting on NF-κB/Rel pathways to protect oxidative injury. In addition, decreases in mRNA expression levels of proinflammatory cytokines indicate that the HGYGT may relieve the symptoms of coronavirus infections.

## 1. Introduction

The number of infectious diseases caused by coronaviruses has recently increased. The severe acute respiratory syndrome coronavirus 1 (SARS-CoV-1) led to a pandemic in 2002, the Middle East respiratory syndrome (MERS)-CoV in 2012, and the SARS-CoV-2 in 2019. Coronaviruses are divided into four types: alpha, beta, gamma, and delta. Human CoV (HCoV) belongs to the genera *Alphacoronavirus* and *Betacoronavirus*. Types 229E and NL63 are Alphacoronaviruses. OC43, HKU1, SAR-CoV-1, MER-CoV, and SAR-CoV-2 are Betacoronaviruses. A novel CoV (2019-nCoV; SAR-CoV-2), identified in January 2020, resulted in respiratory symptoms and had spread worldwide. The recent coronavirus infection, named coronavirus disease 2019

(COVID-19) by the World Health Organization, has led to a global pandemic.

The COVID-19 Korean Medicine Treatment Recommendation, written based on the National Health Commission of the People's Republic of China's treatment plan, recommends herbal medicine treatment at the appropriate time. Some guidelines recommend that uninsured herbal extracts are administered for symptomatic relief. However, in Korea, uninsured herbal extracts are generally perceived to be ineffective compared with packed herbal medicines. Therefore, we determined the effectiveness of an uninsured herbal extract for the treatment of COVID-19.

Hyunggaeyungyo-tang (HGYGT) is an herbal medicine composed of 13 herbs (Table 1). HGYGT is widely

TABLE 1: Composition of HGYGT.

Scientific name	Amount (g)
<i>Schizonepeta tenuifolia</i> Briquet (KP)	0.5
<i>Scutellaria baicalensis</i> Georgi (KP)	0.5
<i>Saposhnikovia divaricata</i> Schischkin (KP)	0.5
<i>Angelica gigas</i> Nakai (KP)	0.5
<i>Poncirus trifoliata</i> Rafinesque (KP)	0.5
<i>Paeonia lactiflora</i> Pallas (KP)	0.5
<i>Glycyrrhiza uralensis</i> Fischer (KP)	0.5
<i>Cnidium officinale</i> Makino (KP)	0.5
<i>Angelica dahurica</i> Bentham et Hooker f (KP)	0.83
<i>Gardenia jasminoides</i> Ellis (KP)	0.5
<i>Platycodon grandiflorum</i> A. De Candolle (KP)	0.83
<i>Forsythia suspensa</i> Vahl (KP)	0.5
<i>Bupleurum falcatum</i> Linné (KP)	0.83

HGYGT: Hyunggaeyungyo-tang; KP: Korean Pharmacopeia.

prescribed in patients with anhidrosis, excessive thirst, excessive sputum, fever, or sore throat. It has been reported that 88% of patients with COVID-19 had fever, 65% had dyspnea, and 60% had a cough [1]. HGYGT is prescribed for these symptoms. We confirmed the antiviral effect of HGYGT using a cell line infected with OC43, a relatively safe *Betacoronavirus*.

Protein kinase RNA-activated (PKR) is one of four mammalian serine-threonine kinases that primarily react to double-stranded RNA (dsRNA) during a viral infection and phosphorylate the eukaryotic initiation factor 2 $\alpha$  (eIF2 $\alpha$ ) translation initiator. The phosphorylation of eIF2 $\alpha$  inhibits the translation of viral mRNAs, ceasing viral replication [2]. In addition, dsRNA is a potent inducer of type I IFN, which produces interferon stimulated genes (ISGs) and forms a protective antiviral state [3]. Virus infection produces reactive oxygen specifications (ROS), which causes virus replication and oxidative injury. [4] We identified the presence of immune-related proteins such as PKR, phosphorylated PKR (pPKR), eIF2, and phosphorylated eIF2 $\alpha$  (peIF2 $\alpha$ ) using immunocytochemistry and measured the expression of proinflammatory cytokines and ISGs to confirm and understand the antiviral effects of HGYGT in A549 cells infected with human coronaviruses.

## 2. Materials and Methods

**2.1. Reagents and Instruments.** The HGYGT used in this experiment was purchased from Hanpoong Pharm. (Jeonju, Korea). The amount of HGYGT's validity was calculated to control the concentration of the active ingredient. HGYGT was diluted with physiological saline to 100  $\mu\text{g}/\text{mL}$ .

The reagents used are TRIsure (Bioline, England), SYBR (Bioline, England), reverse transcriptase (Thermo Fisher Scientific, USA), dNTP (Takara, Japan), DNase (Takara, Japan), RNase inhibitor (Takara, Japan), protease inhibitor (Takara, Japan), primary antibody (Cell Signaling Technology, USA), secondary antibody (Thermo Fisher Scientific, USA), sodium acetate (Invitrogen, USA), and ethanol (Sigma, Germany).

The devices used are RT-PCR (Thermo Fisher Scientific, USA), microreader (Thermo Fisher Scientific, USA), PCR machine (Thermo Fisher Scientific, USA), and ChemiDoc (Thermo Fisher Scientific, USA).

**2.2. Cell Culture.** A549 cells (Korean Cell Line Bank, Korea) were cultured in RPMI medium (Welgene, Korea) and 10% fetal bovine growth serum (RMBio, USA). The cells were cultured at 37°C in a humidified atmosphere containing 5% CO<sub>2</sub>.

**2.3. Virus Infection.** OC43 (1.0 MOI) was added to 5  $\times$  10<sup>5</sup> A549 cells, and the cells were incubated for three days. Cells were then treated with HGYGT (100  $\mu\text{g}/\text{mL}$ ) or deionized, distilled water (DW). The cells were cultured for 72 h prior to RNA extraction.

**2.4. SRB Viability Assay.** Two days after drug treatment, the cells were fixed during 1 hr with 10% TCA solution, washed twice with DPBS, and dried at room temperature. The cells were stained with a 0.05% SRB solution. The stained cells were washed four times with 1% acetic acid and dried at room temperature. After washing four times with DPBS, the cells were then reconstituted 1 hr at room temperature using 10 mM Tris (pH = 10.5). The supernatant of Tris washed samples are analyzed with a microplate reader at an absorbance of 510 nm.

**2.5. RNA Extraction.** The total RNA was extracted using TRIsure (Bioline, England). Prepared cells were distributed into an 8 pi medium consisting of 1  $\times$  10<sup>6</sup> cells on 100 pi plates. A549-OC43 cells (OC43 group) and A549-OC43 cells treated with HGYGT (HGYGT group) were cultured for 72 h. All prepared groups were incubated for 5 min at room temperature before treatment with 1 mL of TRIsure per 5  $\times$  10<sup>5</sup> cells. The lysate was passed several times with a pipette tip. After incubation for 5 min at room temperature, chloroform was added, and the mixture was vortexed for 15 min and then centrifuged for 1 h at 15,000 rpm. After the supernatant was discarded, the pellet was blended with cold isopropyl alcohol to precipitate the RNA. The sample was incubated at room temperature for 10 min and centrifuged at 12,000 rpm at 4°C for 10 min. The pellet was washed using 75% ethanol, air-dried, and dissolved in PCR water. To remove the genetic DNA, purified nucleic acids were treated with DNA enzyme I (Takara, Japan). RNA was reverse-transcribed using RevertAid reverse transcriptase (Thermo Fisher Scientific, USA). The sample was centrifuged for 10 min at 12,000 rpm and room temperature, and the supernatant was discarded. After it was washed twice with 75% ethanol and dried, the pellet was dissolved in DW.

**2.6. cDNA Synthesis and RT-PCR.** For reverse transcription (RT) reactions, PCR was performed with 800 ng of total RNA prepared with 1  $\mu\text{L}$  of random primer. The sample was denatured at 65°C for 5 min, and then, the temperature

dropped to 4°C before 4  $\mu$ L of a 10 mM dNTP mixture and 1  $\mu$ L of reverse transcriptase were added with 1  $\mu$ L RNase inhibitor (20 U/ $\mu$ L) and 4  $\mu$ L 5 $\times$ RT buffer (250 mM Tris-HCl, pH = 8.3, 375 mM KCl, and 15 mM MgCl<sub>2</sub>). PCR was performed at 25°C for 10 min, at 42.5°C for 60 min, and at 70°C for 10 min. RT-PCR (Bio-Rad, USA) was performed using synthesized cDNA, forward/reverse primers, and SensiFAST SYBR Lo-Rox Kit (Bioline, England). The sequences of primers used in the experiment are presented in Table 2. The forward/reverse primer mixture (2  $\mu$ L at 3  $\mu$ M) was combined with 7.5  $\mu$ L SYBR, 4.5  $\mu$ L DW, and 1  $\mu$ L cDNA. In addition, predenaturation was performed for 40 cycles at 5 min each at 95°C, 40 cycles at 95°C, and 1 min at 60°C. The Cq values were calculated.

**2.7. Immunocytochemistry.** The cells were washed twice with PBS and fixed in 4% paraformaldehyde for 15 min at room temperature. Then, the cells were permeabilized with 0.1% Triton X-100 in BSA buffer and blocked for 1 h at room temperature. Cells were incubated with primary antibodies diluted with 1% BSA for 2 h and then washed four times with 0.1% (v/v) Tween-20 in PBS and incubated with Alexa Fluor-conjugated secondary antibodies. The cells were imaged using a Zeiss LSM 760 confocal microscope with a C-Apochromat 20x objective lens (NA = 1.40). PKR and pPKR primary antibodies were purchased from Santa Cruz Biotechnology; eIF2 $\alpha$  and peIF2 $\alpha$  antibodies were obtained from Cell Signaling Technology.

**2.8. Statistical Analysis.** Variables are expressed as mean  $\pm$  SEM. Unpaired one-tailed Student's *t*-tests were used to compare the data. Statistical significance was set at  $p < 0.05$ .

### 3. Results

**3.1. OC43 mRNA Expression.** The OC43 mRNA expression was significantly higher in the OC43 group ( $1.019 \pm 0.1413$ ) than in the HGYGT group ( $0.4205 \pm 0.07611$ ) ( $p < 0.05$ ) (Table 3; Figure 1).

**3.2. Cell Visualizing.** Although the difference was not significant, the expression of PKR was higher in the cells treated with OC43 than cells treated with both OC43 and HGYGT. The expression of pPKR was significantly increased in the cells treated only with OC43 compared with the expression in cells treated with both OC43 and HGYGT. The expression of pPKR in the HGYGT group and uninfected A549 cells was not significantly different (Figure 2). The expression of peIF2 $\alpha$  was significantly higher in the control group than in the cells that were infected with OC43 and treated with HGYGT (Figures 3 and 4).

**3.3. Cell Viability.** The viabilities of cells treated with 100  $\mu$ g/mL, 200  $\mu$ g/mL, 300  $\mu$ g/mL, 400  $\mu$ g/mL, and 500  $\mu$ g/mL HGYGT were 100.891%, 97.4155%, 98.3408%, 100.627%, and 103.914%, respectively. There are no side effects in drug treatment (Figure 5).

**3.4. mRNA Expression.** The expressions of interleukin-1 (IL-1), tumor necrosis factor- $\alpha$  (TNF- $\alpha$ ), cyclooxygenase-2 (COX-2), and nuclear factor kappa-light-chain-enhancer of activated B cells (NF- $\kappa$ B) mRNA were significantly higher in the OC43 group than in the control group (Table 3; Figure 6). The expressions of IL-1 mRNA (OC43:  $27.75 \pm 1.868$ ; HGYGT:  $21.92 \pm 0.6333$ ;  $p < 0.05$ ), TNF- $\alpha$  mRNA (OC43:  $225.8 \pm 24.08$ , HGYGT:  $166.7 \pm 8.045$ ;  $p < 0.05$ ), COX-2 mRNA (OC43:  $10.89 \pm 0.8811$ ; HGYGT:  $6.609 \pm 0.3086$ ;  $p < 0.05$ ), and NF- $\kappa$ B mRNA (OC43:  $6.482 \pm 1.039$ , HGYGT:  $3.807 \pm 0.07861$ ;  $p < 0.05$ ) were significantly higher in cell infected with OC43 than in cells that were infected with OC43 and treated HGYGT (Table 3; Figure 6).

The expressions of Interferon Alpha Inducible Protein 6 (IFI6), IFI44, IFI44L, IFI27, Interferon Regulatory Factor 7 (IRF7), 2'-5'-Oligoadenylate Synthetase Like (OASL), and ISG15 mRNA were significantly higher in the OC43 group than in the control group (Table 3, Figure 7). The expressions of IFI6 mRNA (OC43:  $150.5 \pm 15.18$ ; HGYGT:  $84.61 \pm 7.541$ ;  $p < 0.01$ ), IFI44 mRNA (OC43:  $1413 \pm 169.2$ ; HGYGT:  $761.7 \pm 49.3$ ;  $p < 0.05$ ), IFI44L mRNA (OC43:  $137.1 \pm 4.453$ ; HGYGT:  $98.37 \pm 2.426$ ;  $p < 0.001$ ), IFI27 mRNA (OC43:  $506.2 \pm 48.8$ ; HGYGT:  $328 \pm 29.63$ ;  $p < 0.05$ ), IRF7 mRNA (OC43:  $7.599 \pm 0.6307$ ; HGYGT:  $5.222 \pm 0.7767$ ;  $p < 0.05$ ), OASL mRNA (OC43:  $86.96 \pm 1.575$ ; HGYGT:  $59.74 \pm 2.015$ ;  $p < 0.001$ ), and ISG15 mRNA (OC43:  $71.27 \pm 4.874$ ; HGYGT:  $48.62 \pm 4.098$ ;  $p < 0.05$ ) were significantly higher in cells that were only infected with OC43 than in infected cells treated with HGYGT (Table 3, Figure 7).

The expressions of I $\kappa$ B kinase (IKK) and inducible nitric oxide synthase (iNOS) mRNA were significantly higher in the OC43 infected cells than in the control group (Table 3, Figure 8). The expressions of IKK mRNA (OC43:  $2.6 \pm 0.0503$  HGYGT:  $1.566 \pm 0.1109$ ;  $p < 0.0001$ ) and iNOS mRNA (OC43:  $2.195 \pm 0.05391$ ; HGYGT:  $1.372 \pm 0.02985$ ;  $p < 0.0001$ ) were significantly higher in the OC43-infected cells than in HGYGT-treated infected cells (Table 3, Figure 8).

### 4. Discussion

In December 2019, a number of pneumonia cases of unknown origin were diagnosed in Wuhan City, Hubei Province, China. From this pneumonia, a coronavirus with new genetic information, which has not yet been identified, was detected [5]. The World Health Organization named the virus SARS-CoV-2 as COVID-19 and declared a global pandemic [6]. From the beginning of the outbreak to March 23, 2021, 123,676,223 patients were infected with the virus worldwide, and 2,722,912 patients died.

SARS-CoV-2 belongs to the Coronaviridae family, *Betacoronavirus* genus, and *Sarbecovirus* subgenus. Betacoronaviruses include HCoV-OC43, HCoV-HKU1, SARS-CoV-1, MERS-CoV, and SARS-CoV-2. The SARS-CoV-1 virus infected more than 8,000 people and killed 774 in Guangdong, China from 2002 to 2003. The MERS-CoV virus infected 2,499 people and killed 861 in the Middle East from 2012 to 2019 [7, 8].

TABLE 2: Primer sequences used in RT-PCR.

Target gene	Primer	Nucleic acid sequence
OC43	Forward	5'-AGC AAC CAG GCT GAT GTC AAT ACC-3'
	Reverse	5'-AGC AGA CCT TCC TGA GCC TTC AAT-3'
IL-1	Forward	5'-CCA CAG ACC TTC CAG GAG AAT G-3'
	Reverse	5'-GTG CAG TTC AGT GAT CGT ACA GG-3'
TNF- $\alpha$	Forward	5'-CTC TTC TGC CTG CTG CAC TTT G-3'
	Reverse	5'-ATG GGC TAC AGG CTT GTC ACT C-3'
COX-2	Forward	5'-TCC AAA TGA GAT TGT GGG AAA ATT GCT-3'
	Reverse	5'-AGA TCA TCT CTG CCT GAG TAT CTT-3'
NF- $\kappa$ B	Forward	5'-GCA GCA CTA CTT CTT GAC CAC C-3'
	Reverse	5'-TCT GCT CCT GAG CAT TGA CGT C-3'
IFI6	Forward	5'-TGC TAC CTG CTG CTC TTC AC-3'
	Reverse	5'-CGA GCT CTC CGA GCA CTT TT-3'
IFI44	Forward	5'-CTG ATT ACA AAA GAA GAC ATG ACA GAC-3'
	Reverse	5'-AGG CAA AAC CAA AGA CTC CA-3'
IFI44L	Forward	5'-GTG GAT GAT TGC AGT GAG GTT-3'
	Reverse	5'-AAT ATC CTT CAT GGG GTC CAG-3'
IFI27	Forward	5'-ATC AGC AGT GAC CAG TGT GG-3'
	Reverse	5'-TGG CCA CAA CTC CTC CAA TC-3'
IRF7	Forward	5'-CTG TGG ACA CCT GTG ACA CC-3'
	Reverse	5'-TGC CCT CTC AGG AGC CAA-3'
OASL	Forward	5'-GCG GAG CCC ATC ACG GTC AC-3'
	Reverse	5'-AGG ACC ACC GCA GGC CTT GA-3'
ISG15	Forward	5'-CTC TGA GCA TCC TGG TGA GGA A-3'
	Reverse	5'-AAG GTC AGC CAG AAC AGG TCG T-3'
IKK	Forward	5'-CCA CCC AGT TCC ACA AGT CT-3'
	Reverse	5'-CCT CCA CTG CGA ATA GCT TC-3'
iNOS	Forward	5'-AGA CTG GAT TTG GCT GGT CCC TCC-3'
	Reverse	5'-AGA ACT GAG GGT ACA TGC TGG AGC C-3'

SARS-CoV-2 is a positive-sense single-stranded RNA (ssRNA) virus, enclosed in an 80–220 nm envelope [9]. The virus recognizes a specific protein in the host cell membrane and binds to it, resulting in absorption by the cell. After the virus and the host cell are fused, the uncoated virus RNA invades the host cell. The RNA is replicated using host cell ribosomes and enzymes, and capsids are synthesized. Viruses formed by viral proteases are fused with the host cell membrane and released externally via budding (Figure 9). Antiviral drugs aim to phase out the life cycle of the virus to weaken or extinguish the invading virus by interfering with RNA transcription or inhibiting virus budding [10].

Clinical signs of COVID-19 typically begin within one week after infection and include persistent fever, cough, nasal congestion, fatigue, and other symptoms of upper respiratory infections. Symptoms of the gastrointestinal tract have also been reported, and some cases are asymptomatic [11]. Symptoms may progress to difficulty breathing or extreme chest pain related to pneumonia, decreased oxygen saturation, and physiological changes observed through imaging, such as chest X-ray or CT [12].

According to a study by Son et al. [13], 58.19% of Korean medicine doctors use uninsured herbal extracts. Insured herbal extracts are widely prescribed due to the low cost to patients but differ from packaged herbal medications because they contain extracts of a single herb [14]. For this

reason, uninsured herbal extracts, which are most similar to packed herbal medicines, are widely prescribed despite the cost burden of patients. In this study, uninsured herbal extracts were used for standardization and quality control of drugs.

HGYGT is listed in the Man-Byeong-Hoi-Chun of the Ming Dynasty, composed of 13 substances (Table 1). The HGYGT used in this study contains 0.5 g of *Schizonepeta tenuifolia* Briquet, *Scutellaria baicalensis* Georgi, *Saposhnikovia divaricata* Schischkin, *Angelica gigas* Nakai, *Poncirus trifoliata*, *Rafinesque*, *Paeonia lactiflora* Pallas, *Glycyrrhiza uralensis* Fischer, *Cnidium officinale* Makino, *Gardenia jasminoides* Ellis, *Forsythia suspensa* Vahl and 0.83 g of *Angelica dahurica* Bentham et Hooker f, *Platycodon grandiflorum* A. De Candolle, and *Bupleurum falcatum* Linné. HGYGT is widely used to treat otolaryngeal diseases, including otitis media [15]. Previous studies regarding HGYGT have reported a genotoxicity evaluation [16], antiallergic effects [17], anti-inflammatory effects through NF- $\kappa$ B activation control [18], antioxidant and anti-inflammatory effects through the reduction of iNOS and cytokine production [19], inhibition of inflammatory cell activation, and improvement of immune control [20].

PKR, also known as eukaryotic translation initiation factor 2- $\alpha$  kinase 2 (EIF2AK2), is autophosphorylated by dsRNA in infected cells, leading to an immune response [21].

TABLE 3: mRNA expression.

mRNA	Expression in control group	Expression in OC43 group ( <i>p</i> value vs. control)	Expression in HGYGT group ( <i>p</i> value vs. OC43)
OC43		1.019 ± 0.1413	0.4205 ± 0.07611 *0.0102
IL-1	1.002 ± 0.04936	27.75 ± 1.868 ****<0.0001	21.92 ± 0.6333 *0.0209
TNF- $\alpha$	1.054 ± 0.2352	225.8 ± 24.08 ***0.0004	166.7 ± 8.045 *0.0401
COX-2	1.021 ± 0.1516	10.89 ± 0.8811 ***0.0002	8.609 ± 0.3086 *0.0356
NF- $\kappa$ B	1.009 ± 0.09722	6.482 ± 1.039 **0.0032	3.807 ± 0.07861 *0.0311
IFI6	1.026 ± 0.1712	150.5 ± 15.18 ***0.0003	84.61 ± 7.541 **0.0089
IFI44	1.071 ± 0.2847	1413 ± 169.2 ***0.0006	761.7 ± 49.3 *0.0105
IFI44L	1.009 ± 0.09376	137.1 ± 4.453 ***<0.0001	98.37 ± 2.426 ***0.0008
IFI27	1.002 ± 0.03935	506.2 ± 48.8 ***0.0002	328 ± 29.63 *0.0177
IRF7	1.009 ± 0.09585	7.599 ± 0.6307 ***0.0002	5.222 ± 0.7767 *0.0382
OASL	1.003 ± 0.05799	86.96 ± 1.575 ***<0.0001	59.74 ± 2.015 ***0.0002
ISG15	1.004 ± 0.06054	71.27 ± 4.874 ***<0.0001	48.62 ± 4.098 *0.0118
IKK	1.004 ± 0.06449	2.6 ± 0.0503 ****<0.0001	1.566 ± 0.1109 ****<0.0001
INOS	1.002 ± 0.04371	2.195 ± 0.05391 ****<0.0001	1.372 ± 0.02985 ****<0.0001

Values are presented as mean  $\pm$  SEM ( $n=3$ ) (\* $p < 0.05$ ; \*\* $p < 0.01$ ; \*\*\* $p < 0.001$ ; \*\*\*\* $p < 0.0001$ ).

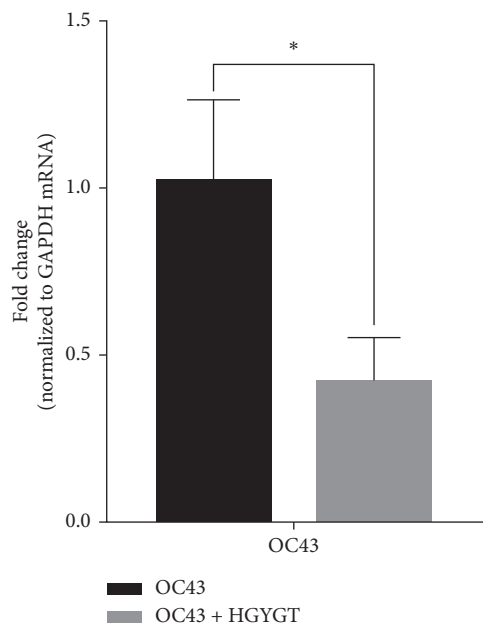


FIGURE 1: OC43 mRNA expression in A549 cells. mRNA expression is measured using quantitative real-time PCR and presented as mean  $\pm$  SD ( $n=3$ ). OC43: cells treated with OC43; OC43 + HGYGT: cells treated with OC43 and HGYGT (100  $\mu$ g/mL) (\* $p < 0.05$ ).

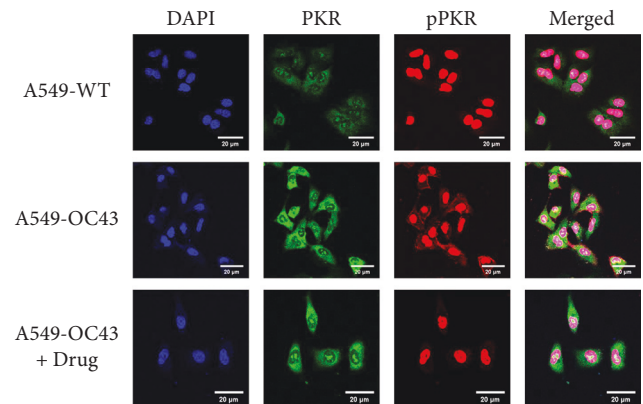


FIGURE 2: Visualization of PKR and pPKR expression. It used a Zeiss LSM 760 confocal microscope with a C-Apochromat 20x objective lens. Although the difference was not significant, the expression of PKR was increased in the "A549-OC43" than in the "A549-OC43 + drug." In the case of pPKR, the expression level was significantly increased in the "A549-OC43" than in the "A549-OC43 + drug." There was no significant difference between the "A549-OC43 + drug" and the "A549-WT" (A549-WT: A549 cells with no treatment; A549-OC43: A549 cells treated with OC43; A549-OC43 + drug: A549 cells treated with OC43 and HGYGT).

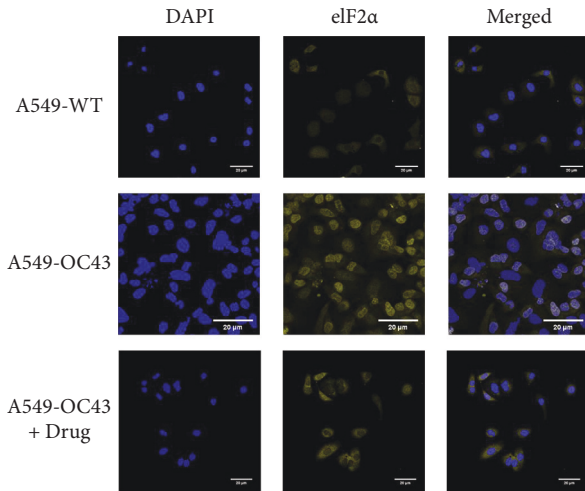


FIGURE 3: Visualization of eIF2 $\alpha$  expression. It used a Zeiss LSM 760 confocal microscope with a C-Apochromat 20x objective lens. The expression level of eIF2 $\alpha$  significantly increased in the “A549-OC43” than in the “A549-OC43 + drug” (A549-WT: A549 cells with no treatment; A549-OC43: A549 cells treated with OC43; A549-OC43 + drug: A549 cells treated with OC43 and HGYGT).

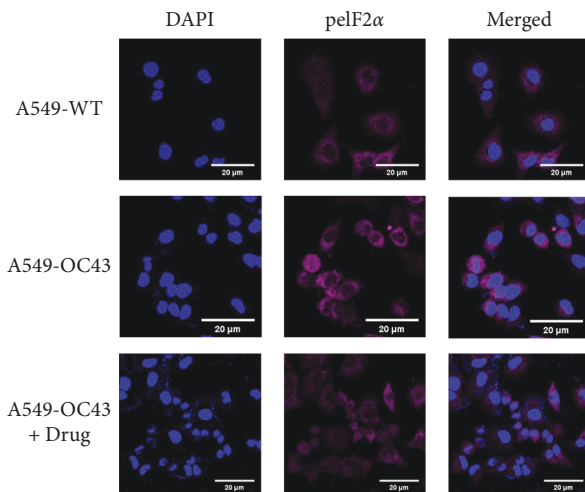


FIGURE 4: Visualization of pEIF2 $\alpha$  expression. It used a Zeiss LSM 760 confocal microscope with a C-Apochromat 20x objective lens. The expression level of pEIF2 $\alpha$  significantly increased in the “A549-OC43” than in the “A549-OC43 + drug” (A549-WT: A549 cells with no treatment; A549-OC43: A549 cells treated with OC43; A549-OC43 + drug: A549 cells treated with OC43 and HGYGT).

pPKR is activated to inhibit global translation by preventing the transition of eIF2 to eIF2B [22]. Existing studies have reported that PKR is a signaling sensor for cellular metabolism [2]. The change in pPKR is proportional to the change in dsRNA. In this study, the expression of pPKR decreased as the amount of dsRNA decreased (Figure 2). Decrease of dsRNA expression inhibits the phosphorylation of PKR, thus inhibiting the activation of eIF2 $\alpha$ . This reduces global translation and reduces protein synthesis (Figure 9). Recently, it has been reported that SARS-CoV-2 activates pPKR [23]. In this study, we found that HGYGT could block

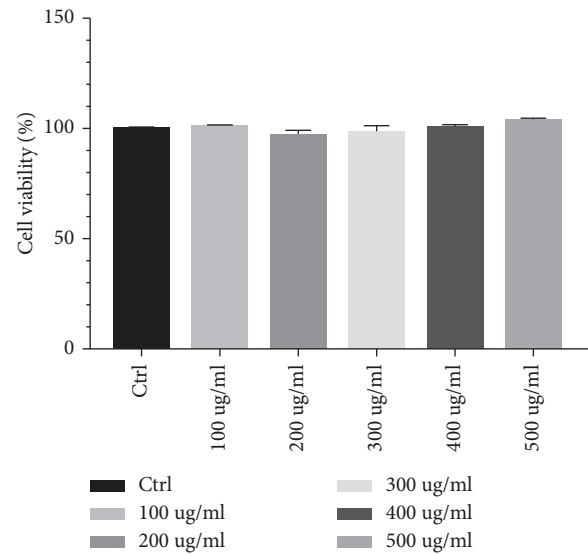


FIGURE 5: SRB assay of HGYGT in A549 cells. Cell viability was assessed by SRB assay at concentrations of 100  $\mu\text{g}/\text{mL}$ , 200  $\mu\text{g}/\text{mL}$ , 300  $\mu\text{g}/\text{mL}$ , 400  $\mu\text{g}/\text{mL}$ , and 500  $\mu\text{g}/\text{mL}$ . The results were calculated as a percentage for the control group and presented as mean  $\pm$  SEM.

phosphorylation of PKR with a decrease of virus RNA expression. This result signifies that HGYGT could be used as a drug to help treat COVID-19.

We confirmed that IFI6, IFI44, IFI44L, IFI27, IRF7, OASL, and ISG15 mRNA expressions were decreased in cells treated with HGYGT compared with those that were not treated with HGYGT (Figure 7). The reduced expressions of these proteins may affect the inactivation of type I interferon (IFN) pathway (Figure 9). Type 1 IFN pathway is a defense mechanism that induces an innate immune response, and excessive production of IFN- $\alpha/\beta$  can lead to the development of autoimmune diseases [24]. The reduction of ISGs that involved in type 1 IFN with HGYGT means that it could be used for the treatment of various immune and inflammatory diseases. Previous studies on hepatitis C virus and RNA viruses have reported that IFI44, IFI44L, and IRF7 are involved in translation [25]. In particular, IFI44L has been reported to be directly involved in the IFN response and acts as a regulator of antiviral responses [26]. It has been reported that IFI27 is involved in replication [27] and OASL is involved in translation [25] and replication [28].

SARS-CoV-2 promotes excessive ROS. As ROS increases, H<sub>2</sub>O<sub>2</sub> accumulates in tissues. The increase in ROS level promotes viral replication and causes oxidative inflammation and cell apoptosis due to DNA damage. Recent studies have reported that catalase regulates cytokine in COVID-19, protects oxidative injuries, and inhibits replication of SARS-CoV-2 [29]. Viral infection increases free radicals, including nitrite oxide (NO), and depletes antioxidants [30]. RNA viruses cause oxidative stress, presumably due to the production of ROS in mitochondrial dysfunction, which occurs during virus infection with cells [31]. The production of iNOS involved in the oxidative injury involves activation of NF- $\kappa\text{B}/\text{Rel}$  [32]. Other studies have reported that inhibiting NF- $\kappa\text{B}$  pathways reduces iNOS

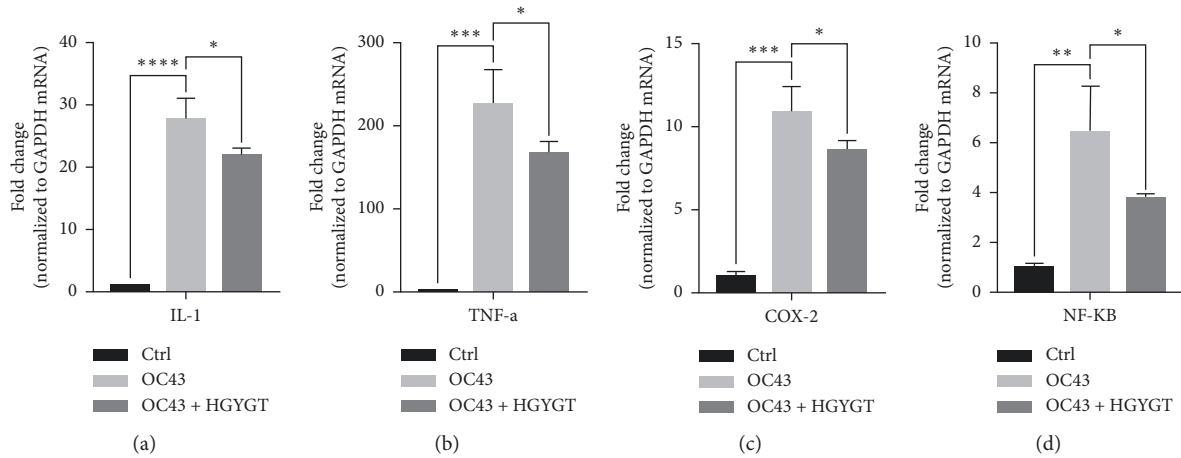


FIGURE 6: Proinflammatory cytokine mRNA expression in A549 cells. mRNA expression is measured using quantitative real-time PCR presented as mean  $\pm$  SD ( $n = 3$ ). Ctrl: cells with no treatment; OC43: cells treated with OC43; OC43 + HGYGT: cells treated with OC43 and HGYGT (100  $\mu$ g/mL) (\*  $p < 0.05$ , \*\*  $p < 0.01$ , \*\*\*  $p < 0.001$ , \*\*\*\*  $p < 0.0001$ ).

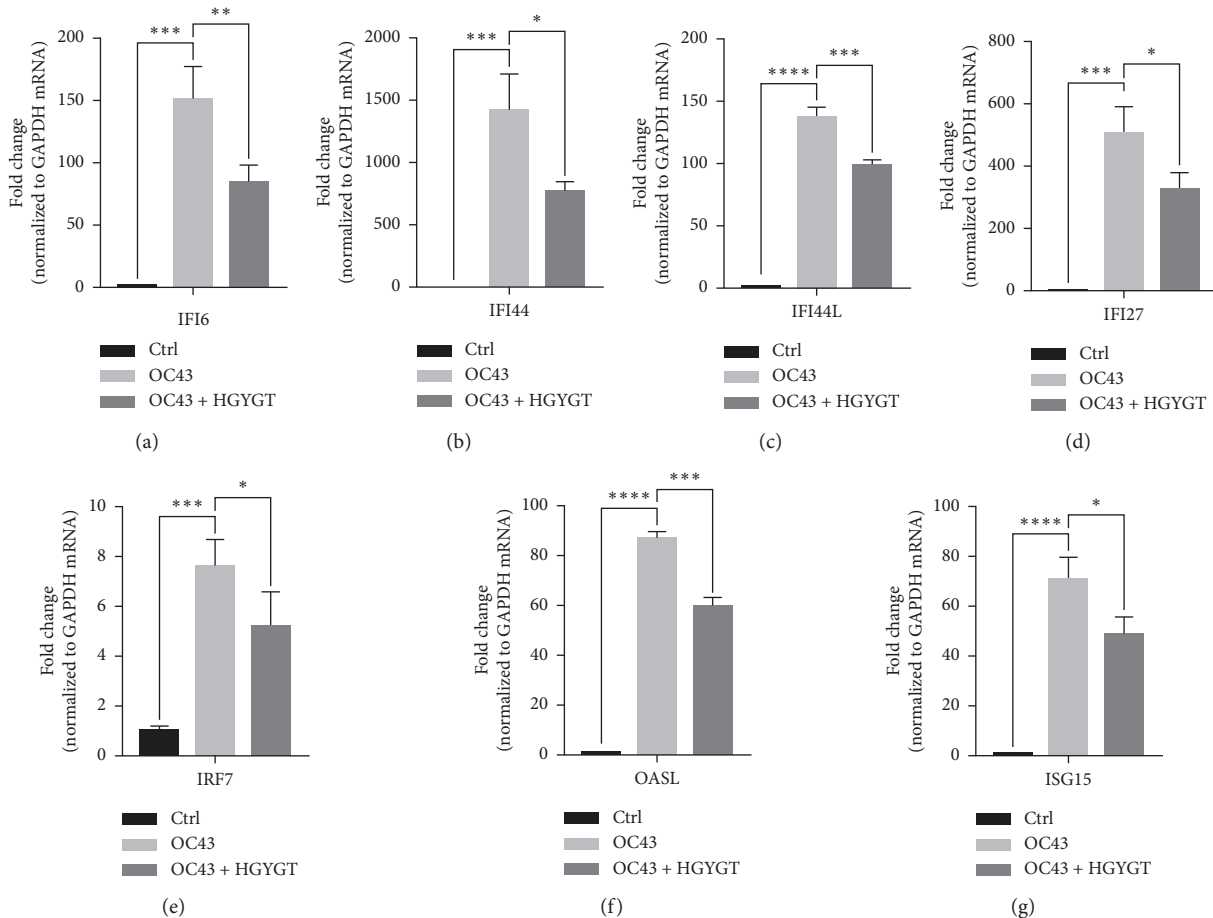


FIGURE 7: ISG mRNA expression in A549 cells. mRNA expression is measured using quantitative real-time PCR and presented as mean  $\pm$  S.D. ( $n = 3$ ). Ctrl: cells with no treatment; OC43: cells treated with OC43; OC43 + HGYGT: cells treated with OC43 and HGYGT (100  $\mu$ g/mL) (\*  $p < 0.05$ ; \*\*  $p < 0.01$ ; \*\*\*  $p < 0.001$ ; \*\*\*\*  $p < 0.0001$ ).

mRNA and NO synthesis [33]. Both LPS and dsRNA are involved in type 1 IFN production. LPS and dsRNA activates antigen-presenting cells (APCs) via the Toll-like receptor 3

(TLR3) and TLR4 signaling pathway [34]. Previous studies have reported the effect of HGYGT suppressing production of iNOS by reducing NF- $\kappa$ B/Rel in an LPS-induced oxidative

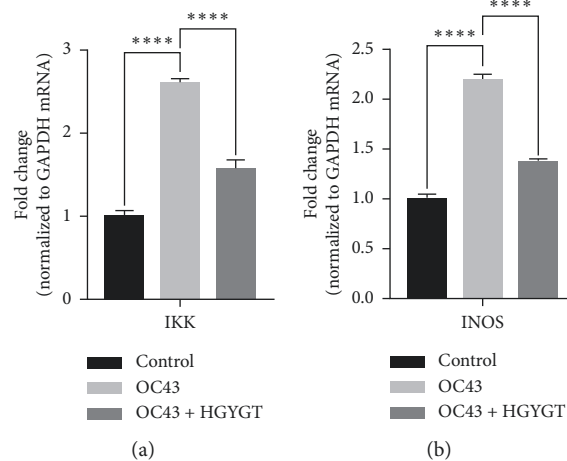


FIGURE 8: IKK and INOS mRNA expression in A549 cells. mRNA expression is measured using quantitative real-time PCR and presented as mean  $\pm$  SD ( $n = 3$ ). Ctrl: cells with no treatment; OC43: cells treated with OC43; OC43 + HGYGT: cells treated with OC43 and HGYGT (100  $\mu$ g/mL) (\*\*\*\*  $p < 0.001$ ).

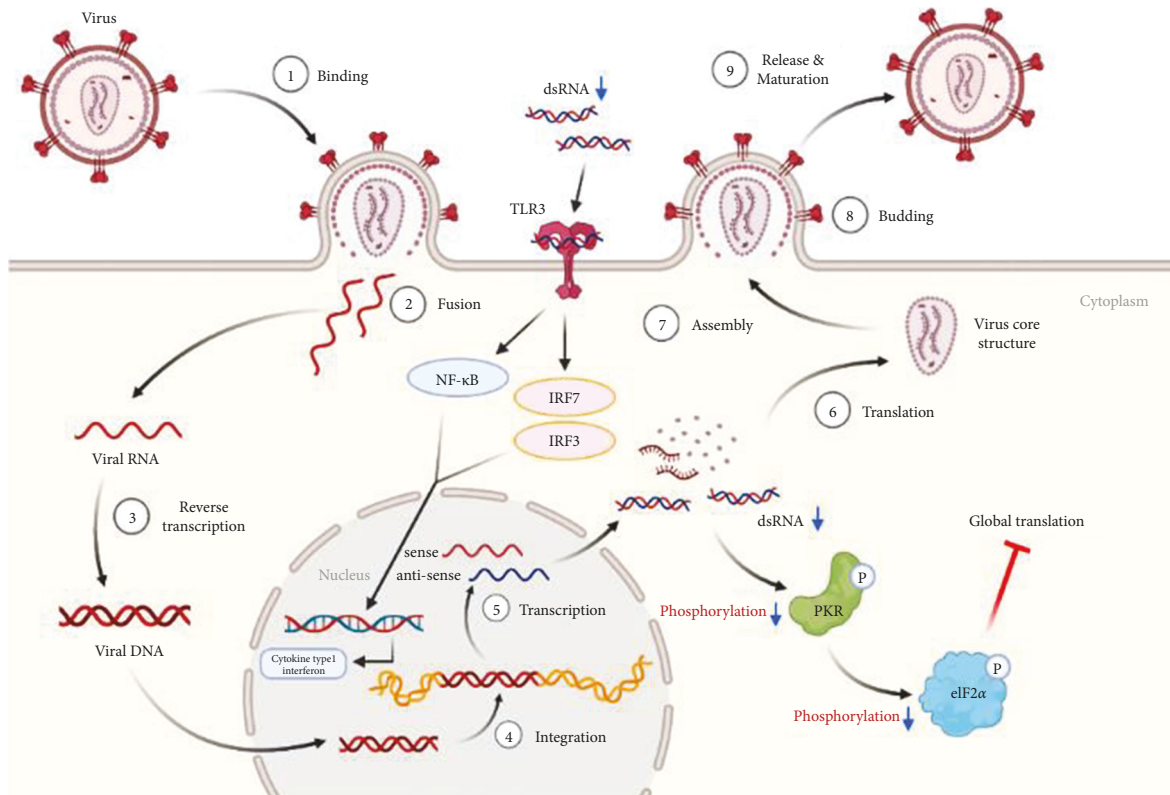


FIGURE 9: Antiviral effect of HGYGT on coronavirus (created with BioRender.com).

injury [35]. Inactivated NF- $\kappa$ B/Rel fails to induce transcription at the NF- $\kappa$ B/Rel bond site in the TATA box of iNOS gene [36]. The expression of iNOS, IKK, and NF- $\kappa$ B was decreased in cells treated with HGYGT compared with those that were not treated with HGYGT (Figure 8). Inflammation with OC43 increases IKK and iNOS mRNA levels in OC43 group. HGYGT reduces IKK activity, and it appears that NF- $\kappa$ B/Rel is inactivated due to reduced I $\kappa$ B

phosphorylation, resulting in iNOS expression reduction. The reduction of IKK and iNOS mRNA levels after HGYGT treatment is believed to be likely to reduce levels of dsRNA and replication of coronavirus by acting on NF- $\kappa$ B/Rel pathways to protect oxidative injury.

The results of this study suggest that HGYGT may have antiviral effects. We evaluated the expression of several proteins and mRNAs to determine the mechanism of



HGYGT. HGYGT reduces the expression of mRNAs for cytokines, such as IL-1, TNF- $\alpha$ , COX-2, NF- $\kappa$ B, iNOS, and IKK, and the expressions of mRNAs for ISGs involved in the type I IFN pathway, resulting in a decreased immune response and fewer clinical symptoms. We suggest that HGYGT of uninsured herbal extracts manufactured by pharmaceutical companies effectively reduces the virus via regulation in NF- $\kappa$ B/Rel pathways and reduces the symptoms of the coronavirus infection. However, our study is limited due to its in vitro design and an insufficient sample size. More studies, including in vivo and clinical studies, are needed to determine the effects of HGYGT on coronavirus infections. The preprint of this manuscript [37] can be found in <https://www.biorxiv.org/content/10.1101/2021.06.02.446680v1>.

## 5. Conclusions

HGYGT reduced the mRNA expression levels of coronavirus and inhibited the phosphorylation of PKR. It reduced mRNA expression level of iNOS and IKK. It means HGYGT may regulate NF- $\kappa$ B/Rel pathways and has an antioxidative effect. HGYGT blocks a series of processes of ISG expression and reduces the inflammatory response in Betacoronavirus-infected A549 cells. Thus, HGYGT acts as a potential therapeutic agent for various clinical symptoms caused by coronavirus.

## Abbreviations

APC:	Antigen-presenting cells
COVID-19:	Coronavirus disease 2019
COX-2:	Cyclooxygenase-2
dsRNA:	Double-stranded RNA
eIF2:	Eukaryotic initiation factor 2
EIF2AK2:	Eukaryotic translation initiation factor 2-alpha kinase 2
HCoV:	Human CoV
HGYGT:	Hyeonggae Yeongyo-tang
IFI:	Interferon alpha inducible protein
IFN:	Interferon
IKK:	I $\kappa$ B kinase
IL:	Interleukin
iNOS:	Inducible nitric oxide synthase
IRF:	Interferon regulatory factor
ISGs:	Interferon stimulated genes
MERS:	Middle east respiratory syndrome
NF- $\kappa$ B:	Nuclear factor kappa-light-chain-enhancer of activated B cells
NO:	Nitrite oxide
OASL:	2'-5'-Oligoadenylate synthetase-like
PKR:	Protein kinase RNA-activated
ROS:	Reactive oxygen species
RT:	Reverse transcription
SARS-CoV:	Severe acute respiratory syndrome coronavirus
ssRNA:	Single-stranded RNA
TLR:	Toll-like receptor

TNF- $\alpha$ : Tumor necrosis factor- $\alpha$ .

## Data Availability

The datasets generated or analyzed in this study are available from the corresponding author upon reasonable request.

## Disclosure

This paper has been submitted under the preprint [37] and can be found at <https://www.biorxiv.org/content/10.1101/2021.06.02.446680v1>.

## Conflicts of Interest

The authors declare that there are no conflicts of interest regarding the publication of this article.

## Acknowledgments

The authors are grateful to the experts for their valuable advice.

## References

- [1] O. J. McElvaney, N. L. McEvoy, O. F. McElvaney et al., "Characterization of the inflammatory response to severe COVID-19 illness," *American Journal of Respiratory and Critical Care Medicine*, vol. 202, no. 6, pp. 812–821, 2020.
- [2] M. A. Garcia, E. F. Meurs, and M. Esteban, "The dsRNA protein kinase PKR: virus and cell control," *Biochimie*, vol. 89, no. 6-7, pp. 799–811, 2007.
- [3] S. J. Poynter and S. J. DeWitte-Orr, "Understanding viral dsRNA-mediated innate immune responses at the cellular level using a rainbow trout model," *Frontiers in Immunology*, vol. 9, p. 829, 2018.
- [4] M. L. Reshi, Y. C. Su, and J. R. Hong, "RNA viruses: ROS-mediated cell death," *International Journal of Cell Biology*, vol. 2014, Article ID 467452, 16 pages, 2014.
- [5] D. Paraskevis, E. G. Kostaki, G. Magiorkinis, G. Panayiotakopoulos, G. Sourvinos, and S. Tsiodras, "Full-genome evolutionary analysis of the novel corona virus (2019-nCoV) rejects the hypothesis of emergence as a result of a recent recombination event," *Infection, Genetics and Evolution: Journal of Molecular Epidemiology and Evolutionary Genetics in Infectious Diseases*, vol. 79, Article ID 104212, 2020.
- [6] World Health Organization, *WHO Director-General's Remarks at the Media Briefing on 2019-nCoV on 11 February 2020* World Health Organization, Geneva, Switzerland, 2020.
- [7] J. Guarner, "Three emerging coronaviruses in two decades," *American Journal of Clinical Pathology*, vol. 153, no. 4, pp. 420–421, 2020.
- [8] T. T. Yao, J. D. Qian, W. Y. Zhu, Y. Wang, and G. Q. Wang, "A systematic review of lopinavir therapy for SARS coronavirus and MERS coronavirus—a possible reference for coronavirus disease-19 treatment option," *Journal of Medical Virology*, vol. 92, no. 6, pp. 556–563, 2020.
- [9] J. A. Englund, Y. J. Kim, and K. McIntosh, "Human coronaviruses, including middle east respiratory syndrome coronavirus," in *Feigin and Cherry's Textbook of Pediatric Infectious Disease*, J. Cherry, G. J. Demmler Harrison, S. L. Kaplan, W. J. Steinbach, and P. J. Hotez, Eds.,

- pp. 1846–1854, Elsevier, Philadelphia, PA, USA, 8th edition, 2019.
- [10] J. M. Parks and J. C. Smith, “How to discover antiviral drugs quickly,” *New England Journal of Medicine*, vol. 382, no. 23, pp. 2261–2264, 2020.
  - [11] W.-j. Guan, Z.-y. Ni, Y. Hu et al., “Clinical characteristics of coronavirus disease 2019 in China,” *New England Journal of Medicine*, vol. 382, no. 18, pp. 1708–1720, 2020.
  - [12] T. P. Velavan and C. G. Meyer, “The COVID-19 epidemic,” *Tropical Medicine and International Health*, vol. 25, no. 3, pp. 278–280, 2020.
  - [13] C. H. Son, Y. H. Kim, and S. Lim, “A study on Korean oriental medical doctors’ use of uninsured herbal extracts and how to promote the insurance coverage of such herbal extracts,” *Korean Journal of Oriental Medicine*, vol. 30, no. 4, pp. 64–78, 2009.
  - [14] S. J. Park, S. H. Kim, K. S. Kim et al., “A quantitative analysis of marker compounds in single herb extracts by the standard of KHP,” *The Korea Journal of Herbology*, vol. 29, no. 3, pp. 35–42, 2014.
  - [15] M. R. Yang, K. S. Jin, H. J. Lee, M. W. Kwon, and E. J. Park, “A clinical study on the therapeutic effect of kamihyunggyeungyotang for pediatric recurrent otitis media with effusion,” *Journal of Pediatrics of Korean Medicine*, vol. 15, no. 2, pp. 87–100, 2001.
  - [16] S. Y. Jee, S. Y. Hwang, J. R. Lee, and S. C. Kim, “A study of genotoxicity test of hyeong-gae-yeon-gyo-tang extract,” *Korea Journal of Herbology*, vol. 22, no. 4, pp. 287–300, 2007.
  - [17] T. S. Yoo, Y. S. Chin, and K. M. Jeong, “Study of the effects of Hyunggaeyeungyotang on the anti-allergic effect in rats and mice,” *The Journal of Pediatrics of Korean Medicine*, vol. 4, no. 1, pp. 19–30, 1990.
  - [18] J.-H. Park and S.-U. Hong, “The effects of hyunggaeyungyotang of suppression of iNOS production on mice with allergic rhinitis,” *The Journal of Korean Oriental Medical Ophthalmology and Otolaryngology and Dermatology*, vol. 25, no. 1, pp. 12–21, 2012.
  - [19] M. J. Kim, J. R. Lee, S. C. Kim, and S. Y. Jee, “Inhibitory effect of hyeonggaeyeungyotang water extract on production of nitric oxide, IL-6 and expression of iNOS, COX-2 in LPS-activated raw 264.7 cells,” *Korean Journal of Oriental Physiology & Pathology*, vol. 21, no. 2, pp. 491–497, 2007.
  - [20] R. Y. Kang, B. K. Park, S. B. Kim, H. J. Choi, and D. H. Kim, “The effects of HYT on various immunological factors related to pathogenesis of allergic dermatitis in NC/Nga mice induced by Biostir AD,” *Journal of Haehwa Medicine*, vol. 18, no. 2, pp. 47–62, 2009.
  - [21] R. C. Patel, P. Stanton, N. M. McMillan, B. R. Williams, and G. C. Sen, “The interferon-inducible double-stranded RNA-activated protein kinase self-associates in vitro and in vivo,” *Proceedings of the National Academy of Sciences*, vol. 92, no. 18, pp. 8283–8287, 1995.
  - [22] E. F. Meurs, Y. Watanabe, S. Kadereit et al., “Constitutive expression of human double-stranded RNA-activated p68 kinase in murine cells mediates phosphorylation of eukaryotic initiation factor 2 and partial resistance to encephalomyocarditis virus growth,” *Journal of Virology*, vol. 66, no. 10, pp. 5805–5814, 1992.
  - [23] Y. Li, D. M. Renner, C. E. Comar et al., “SARS-CoV-2 induces double-stranded RNA-mediated innate immune responses in respiratory epithelial-derived cells and cardiomyocytes,” *Proceedings of the National Academy of Sciences*, vol. 118, no. 6, Article ID e2022643118, 2021.
  - [24] J. Banchereau and V. Pascual, “Type I interferon in systemic lupus erythematosus and other autoimmune diseases,” *Immunity*, vol. 25, no. 3, pp. 383–392, 2006.
  - [25] J. W. Schoggins, S. J. Wilson, M. Panis et al., “A diverse range of gene products are effectors of the type I interferon antiviral response,” *Nature*, vol. 472, no. 7344, pp. 481–485, 2011.
  - [26] M. L. DeDiego, L. Martinez-Sobride, and D. J. Topham, “Novel functions of IFI44L as a feedback regulator of host antiviral responses,” *Journal of Virology*, vol. 93, no. 21, 2019.
  - [27] Y. Itsui, N. Sakamoto, M. Kurosaki et al., “Expressional screening of interferon-stimulated genes for antiviral activity against hepatitis C virus replication,” *Journal of Viral Hepatitis*, vol. 13, no. 10, pp. 690–700, 2006.
  - [28] M. Ishibashi, T. Wakita, and M. Esumi, “2',5'-Oligoadenylate synthetase-like gene highly induced by hepatitis C virus infection in human liver is inhibitory to viral replication in vitro,” *Biochemical and Biophysical Research Communications*, vol. 392, no. 3, pp. 397–402, 2010.
  - [29] M. Qin, Z. Cao, J. Wen et al., “An antioxidant enzyme therapeutic for COVID-19,” *Advanced Materials*, vol. 32, Article ID e2004901, 2020.
  - [30] F. C. Camini, C. C. da Silva Caetano, L. T. Almeida, and C. L. de Brito Magalhães, “Implications of oxidative stress on viral pathogenesis,” *Archives of Virology*, vol. 162, no. 4, pp. 907–917, 2017.
  - [31] A. V. Ivanov, V. T. Valuev-Elliston, O. N. Ivanova et al., “Oxidative stress during HIV infection: mechanisms and consequences,” *Oxidative medicine and cellular longevity*, vol. 2016, Article ID 8910396, 18 pages, 2016.
  - [32] Q. W. Xie, Y. Kashiwabara, and C. Nathan, “Role of transcription factor NF-kappa B/Rel in induction of nitric oxide synthase,” *Journal of Biological Chemistry*, vol. 269, no. 7, pp. 4705–4708, 1994.
  - [33] M. Matsumura, H. Kakishita, M. Suzuki, N. Banba, and Y. Hattori, “Dexamethasone suppresses iNOS gene expression by inhibiting NF-κB in vascular smooth muscle cells,” *Life Sciences*, vol. 69, no. 9, pp. 1067–1077, 2001.
  - [34] K. Hoebe and B. Beutler, “LPS, dsRNA and the interferon bridge to adaptive immune responses: trif, Tram, and other TIR adaptor proteins,” *Journal of Endotoxin Research*, vol. 10, no. 2, pp. 130–136, 2004.
  - [35] J. H. Park, J. C. Kim, and S. U. Hong, “The effects of Hyunggaeyungyotang of suppression of iNOS production on RAW 264.7 cell,” *The Journal of Korean Oriental Medical Ophthalmology & Otolaryngology & Dermatology*, vol. 24, no. 1, pp. 78–85, 2011.
  - [36] C. J. Lowenstein, E. W. Alley, P. Raval et al., “Macrophage nitric oxide synthase gene: two upstream regions mediate induction by interferon gamma and lipopolysaccharide,” *Proceedings of the National Academy of Sciences*, vol. 90, no. 20, pp. 9730–9734, 1993.
  - [37] S. Y. Won, I. C. Seol, H. R. Yoo, and Y. S. Kim, “Antiviral effect of hyunggaeyungyotang on A549 cells infected with human coronavirus,” *BioRxiv*, 2021.